Chapter 3

Secondary Organic Aerosol Formation by Heterogeneous Reactions of Aldehydes and Ketones: A Quantum Mechanical Study*

* This chapter is reproduced by permission from "Secondary Organic Aerosol Formation by Heterogeneous Reactions of Aldehydes and Ketones: A Quantum Mechanical Study" by C. Tong, M. Blanco, W. A. Goddard III, and J. H. Seinfeld, *Environmental Science and Technology*, 40, 2323-2338, 2006.

3.1 Abstract

Experimental studies have provided convincing evidence that aerosol-phase heterogeneous chemical reactions (possibly acid-catalyzed) are involved to some extent in the formation of secondary organic aerosol (SOA). We present a stepwise procedure to determine physical properties such as heats of formation, standard entropies, Gibbs free energies of formation, and solvation energies from quantum mechanics (QM), for various short-chain aldehydes and ketones. We show that quantum mechanical gas-phase Gibbs free energies of formation compare reasonably well with the literature values with a root mean square (RMS) value of 1.83 kcal/mol for the selected compounds. These QM results are then used to determine the equilibrium constants (reported as log K) of aerosol-phase chemical reactions, including hydration reactions and aldol condensation for formaldehyde, acetaldehyde, acetone, butanal, hexanal, and glyoxal. Results are in qualitatively agreement with previous studies. In addition, the QM results for glyoxal reactions are consistent with experimental observations. To our knowledge, this is the first QM study that supports observations of atmospheric particle-phase reactions. Despite the significant uncertainties in the absolute values from the QM calculations, the results are potentially useful in determining the relative thermodynamic tendency for atmospheric aerosol-phase reactions.

3.2 Introduction

Secondary organic aerosol (SOA) formation by gas/particle (G/P) partitioning has traditionally focused on low volatility products. The quantity of SOA formed can be estimated using absorptive or adsorptive G/P partitioning theory which assumes that this quantity is governed strongly by the vapor pressure of the compound as well as the liquid-phase activity coefficient [1-5]. Recent experimental work has suggested that the amount of SOA formed in a number of systems exceeds that based purely on G/P partitioning of low vapor pressure oxidation product [6-10]. Evidence also indicates that relatively volatile oxidation products, especially aldehydes and ketones, are being absorbed into the aerosol phase where they undergo aerosol-phase chemical reactions. The reaction products have relatively low vapor pressures compared to their parent compounds, which leads to additional partitioning from gas to particle phase, and hence, increases the organic particulate material (OPM). Aerosol-phase reactions, such as hydration, polymerization, hemiacetal/acetal formation, and aldol condensation, have been postulated as a means by which low volatility compounds can be formed thereby increasing the amount of OPM formed beyond that due to G/P partitioning of low vapor pressure gas-phase oxidation products alone.

Theoretical studies by Barsanti and Pankow [11] have shown, however, that reactions such as hydration, polymerization, hemiacetal/acetal formation are not thermodynamically favorable under atmospheric conditions. Their results do suggest that aldol condensation may be thermodynamically favorable. These results seem to deviate from experimental observation [9]. On the other hand, they have shown that diol and subsequent oligomer formation are favorable for glyoxal [12], and these findings are

consistent with experiments [13-15] .While the experimental studies have provided convincing evidence that aerosol-phase chemical reactions (possibly acid- catalyzed) are involved to some extent in formation of SOA, uncertainty remains as to the likely aerosol-phase chemical reactions involving absorbed gas-phase organic compounds.

The reactive uptake mechanism for relatively small, volatile organic compounds (short-chain aldehydes and ketones) is not well understood. Hydration is invariably the first step for volatile organics to dissolve into the particle phase, followed by various (possibly acid-catalyzed) reactions such as polymerization, hemiacetal/acetal formation, and aldol condensation. As suggested by Barsanti and Pankow [11], aldol condensation may be the most accessible reaction path for additional OPM formation.

In the current study, we investigate the thermodynamic feasibility of various particle-phase heterogeneous reactions for some common atmospheric carbonyl compounds using quantum mechanical methods. In particular, we consider the hydration reaction and aldol condensation for small, short-chain aldehydes and ketones, such as formaldehyde, acetaldehyde, acetone, butanal, and hexanal. We also include glyoxal in our investigation. The relatively simple structure of glyoxal as well as its clear importance as an atmospheric oxidation product of a number of hydrocarbons makes it an excellent candidate for theoretical study. Recent studies [13-16] have shown aerosol growth by heterogeneous reactions of gas-phase glyoxal. The thermodynamic feasibility of a proposed glyoxal reaction pathway [14] is evaluated in our study. Similar to the studies by Barsanti and Pankow [11, 12], the thermodynamic analysis presented in this work is independent of the actual reaction pathway. The goal is to present a method to identify potential particle-phase reactions that may contribute to atmospheric OPM, and

the extent of OPM contribution if the reactions are kinetically favorable. This study does not yield any information regarding the kinetics; therefore, evidence of additional OPM formation may remain unobservable at short time scales. On the other hand, we focus only on determining the solution-phase equilibrium constant, *K*, which is the governing factor of the overall tendency of the reactions in the particle. Owing to the chemical complexity of atmospheric aerosols, one is often faced with the difficulty in obtaining physical properties for species for which limited experimental data exist. Here we apply novel quantum chemistry methods as an alternative predictive approach, which may reduce the number of parameters/experimental data required.

3.3 Computational Method

In order to calculate equilibrium constants (*K*) of the reactions, the standard Gibbs free energy of a reaction (ΔG^0_r) are needed and can be calculated by the standard Gibbs free energy of formation (ΔG^0_f). It is also related to the equilibrium constant (*K*) according to the fundamental equation

$$\Delta G_r^0 = \sum_j v_j \Delta G_{f,j}^0 = -RT \ln K \qquad (3.1)$$

where v_i is the stoichiometric coefficient for *j* in the reaction, $\Delta G^0_{f,j}$ is the standard Gibbs free energy of formation for *j*. $\Delta G^0_{f,j}$ can be determined using gas-phase heats of formations and standard entropies ($\Delta G^0_{f,j} = \Delta H^0_{f,j} - T\Delta S^0_j$). Then, as illustrated by Figure 3.1, the free energy of reaction in aqueous solution, ΔG^0_r(aq), is related to the gas-phase free energy of reaction, ΔG^0_r(gas) by adding the solvation energies of the species, ΔG^0_s.

$$\Delta G_r^0(\text{aq}) = \Delta G_r^0(\text{gas, 1M}) + \sum_j v_j \Delta G_s^0 \qquad (3.2)$$

All the necessary quantities ($\Delta H^0_{f,j}$, ΔS^0_j and ΔG^0_s) can be determined by QM and the procedure will be described below. It should be noted here that proper standard state conditions should be used for the free energy calculations in equation 3.2. The standard state for gas-phase reactions is 1 atm at 298K while the standard state for aqueous solution is 1 M at 298K. A brief description of the standard state conversion is provided in the Supporting information.

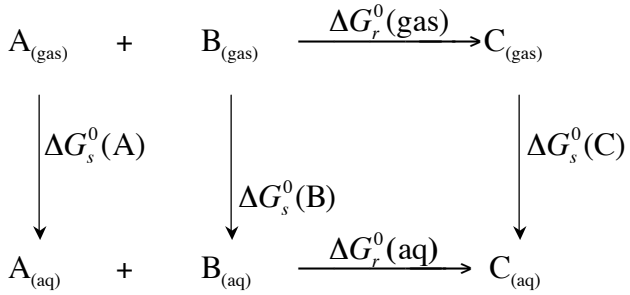

Figure 3.1: Thermodynamic cycle for computation of energy changes of reaction in the gas phase and solution. Adapted from Cramer (2004) [17]

3.3.1 Gas-phase Standard Heats of Formation.

QM calculated standard heats of formation would be the first step to obtain free energies of formation for equation (3.1). QM heats of formation at 298K is given by the equation:

$$\Delta H^0_{f,j}(QM) = E_{elec} + E_{zpe} + \Delta H_{(0-298K)} + \Delta H^*_{298K} \qquad (3.3)$$

To obtain the ground state energy (E_{elec}), the molecules were optimized using DFT/X3LYP, with a fairly large basis set aug-cc-pVTZ(-f) [18] in the gas phase. For molecules with different conformations, geometry optimization using a smaller basic set 6-31g** [19] was carried out to select 4 (or 5) relatively stable conformations. Further optimizations were then performed for the selected structures at the higher level to calculate E_{elec}. The vibrational frequency calculations are performed for the most stable

structure at the HF/631g** level in the gas phase with a scaling factor 0.8992. This scaling factor was determined by comparing the theoretical harmonic vibrational frequencies with the corresponding experimental values utilizing a total of 122 molecules (1066 individual vibrations) and a least-squares approach [20]. The frequency calculations ascertain the structure of the molecules and provide zero point vibrational energy (E_{zpe}), the thermal vibrational, rotational, and translational enthalpy from 0 K to 298 K ($\Delta H_{(0\text{-}298\text{K})}$). The last term in equation 3.3, $\Delta H^*_{298\text{K}}$, allows for corrections between the theoretical heats of formation, referenced to the electrons and nuclei separated an infinite distance, and experimental values, referenced to the elements at standard temperature and pressures. A common reference is the enthalpies of formation for the neutral atoms in the gas phase, so:

$$\Delta H^*_{298K} = \sum_{i=1}^{n} n_i (h_i^0 - h_i^{QM}) \qquad (3.4)$$

where n is the number of elements in the compound, n_i is the number of atoms of each element. h_i^0 is the experimental atomic heats of formation in the gas phase [21], and h_i^{QM} is the theoretical value:

$$h_i^{QM} = E_i^{elec} + \frac{3}{2}RT - PV = E_i^{elec} + \frac{1}{2}RT \qquad (3.5)$$

where E_i^{elec} is the quantum electronic energy, 3/2 RT is the translational energy at 298K and the ideal gas law is applied for PV, R is the gas constant, and T is the temperature.

Large discrepancies can be found between the QM calculated heats of formation using equation 3.3 – 3.5 and the experimental heats of formation. Improvement can be made by applying the correction scheme such as the J2 model of Dunietz et al. [22] to the

enthalpies. The J2 model is based on the generalized valence bond-localized Møller - Plesset method (GVB-LMP2), and it uses a three parameter correction term composed of σ bond and π bond parameters and an additional parameter to account for the difference of lone pairs between the molecule and the separated atoms. Recently, Blanco and Goddard [23] developed a correction scheme closely following the J2 corrections [22], but their "chemical bond" scheme for high level corrections (CBHLC) applies to DFT quantum calculations and only consists of the two σ bond and π bond parameters. Details of the CBHLC scheme are given in the Supporting Information.

All calculations were performed using the Jaguar 6.0 package [24]. QM calculations were carried out using DFT with X3LYP. X3LYP is an extended hybrid density functional that has been shown to be an accurate and practical theoretical method [25-27], with a particularly accurate estimation of van der Waals interactions.

3.3.2 Standard Free Energies of Formation and Equilibrium Constants

Adding the entropy term to the QM gas-phase heats of formation will give us the standard Gibbs free energy, ΔG^{0}_{f}, at 298K:

$$\Delta G^{0}_{f,j} = \Delta H^{0}_{f,j}(QM) - T\left(S_{j,298K}(QM) - \sum_{i=1}^{n} n_i S_{i,298K} \right) \qquad (3.6)$$

where $S_{j,298K}(QM)$ is the entropy of the compound at 298K and $S_{j,298K}$ is the entropy for the elements in their reference states [21]. At this point, we can obtain the gas-phase Gibbs free energies of reaction using equation 3.1. In order to obtain solution-phase energies, the solvation effect is accounted by the free energy of solvation, (ΔG_s^{0}), as shown in Figure 3.1.

3.3.3 Solution phase energy

QM determined solvation energies, ΔG_s^0, for both the parent compounds and reaction products are shown in Table 3.2. Solvation energy (ΔG_s^0) describes the interaction of a solute with a surrounding solvent. Change in entropies due to conformational changes of the molecules from gas phase to aqueous phase is minimized by re-optimization of the compounds at X3LYP/cc-pVTZ(-f) using the implicit continuum solvent model [28-30]. In a continuum model, solute atoms are treated explicitly and the solvent is represented as a continuum dielectric medium. The electrostatic contribution to the solvation free energy is computed using the Poisson-Boltzmann (PB) method (see Supporting Information). The PB equation is valid under conditions where dissolved electrolytes are present in the solvent, but the current implementation of the QM solvation model is confined to zero ionic strength. The effect on the equilibrium constant for reactions in solution with dissolved electrolytes remains unknown because the change in solvation effect due to ionic strength of the solvent varies with species. Although the solvation model is limited to solution zero ionic strength, we can apply the solvation model to any solvent with the proper choice of dielectric constant. Water is chosen in this study because it is often the most important component in aerosols.

3.4 Results and Discussion

Calculated QM free energies of formation in the gas phase, ΔG_f^0 (*QM*), and estimated free energies of formation obtained from the group contribution "Joback method" [31], ΔG_f^0 (*Joback*). Both estimations are compared to the gas-phase literature values [32], and the differences (δG) are calculated (see Table 3.1).

Table 3.1: Quantum calculated free energies of formation. The literature free energies of formation and group contribution (Joback) method estimated values are included for comparison. Absolute errors (δG) are also shown. All values are in kcal/mol

	ΔG_f^0 (*exp*)[a]	ΔG_f^0 (*Joback*) [31]	δG[c]	ΔG_f^0 (*QM*)	δG[d]
Water	-54.60 ± 0.11	--[b]	--	-53.92	0.68
Formaldehyde	-24.51 ± 0.74	--[b]	--	-24.96	-0.45
Acetaldehyde	-31.84 ± 0.96	-31.90	-0.06	-33.68	-1.84
Acetone	-36.14 ± 1.08	-36.91	-0.77	-39.29	-3.16
Butanal	-27.78 ± 0.83	-27.88	-0.10	-29.06	-1.28
Hexanal	-23.90 ± 0.72	-23.86	0.04	-23.72	0.18
Glyoxal	-45.31	-55.67	-10.36	-45.23	0.07
Ethylene glycol	-72.08 ± 2.16	-73.49	-1.40	-69.41	2.67
Hydroxyacetone	-68.07 ± 6.81	-69.59	-1.52	-70.04	-1.97
2,4-pentanedione	-64.37 ± 0.64	-63.68	0.69	-61.77	2.60
Glutaraldehyde	-48.58 ± 2.43	-49.64	-1.06	-46.61	1.97
Cyclopropane carboxylic acid	-58.49 ± 1.75	-71.74	-13.25	-56.80	1.69

a. Gas-phase literature values and uncertainties of free energies of formation, $\Delta G_f^0(exp)$ are obtained from DIPPR database [32].
b. The group contribution Joback method [31] lacks sufficient groups to estimated ΔG_f^0 for water and formaldehyde.
c. $\delta G = \Delta G_f^0(Joback) - \Delta G_f^0(exp)$
d. $\delta G = \Delta G_f^0(QM) - \Delta G_f^0(exp)$.

Group contribution methods are widely used because of their efficiency and accuracy. Barsanti and Pankow [11] found that the estimated ΔG_f^0 by the Joback method agrees with the values from Yaws [33] to ±0.7 kcal/mol (±3 kJ/mol) for a set of compounds including alcohols, aldehydes and ketones. However, as for all predictive methods, group contribution methods are limited by the experimental data that were used in the parameterization, which may be problematic for multi-functional compounds where experimental data are scarce. For the selected 12 compounds, the root mean square (RMS) value for errors between $\Delta G_f^0(Joback)$ and $\Delta G_f^0(exp)$ is 5.80 kcal/mol (vs. 0.90

kcal/mol if we exclude glyoxal and cyclopropane carboxylic acid). Since the CBHLC corrections is extended to include multi-functional oxygenates, the RMS value for the discrepancies between QM ΔG_f^0(gas) and ΔG_f^0(*exp*) is 1.83 kcal/mol for all compounds shown in Table 3.1. Although the RMS deviation for QM ΔG_f^0(gas) is significantly higher (1.90 kcal/mol vs. 0.90 for Joback method when glyoxal and cyclopropane carboxylic acid are excluded), the predictive power of QM methods can be of great use for species that have not been studied experimentally.

Table 3.2: Quantum calculated free energies of formation, ΔG_f^0, and solvation energies, ΔG_s^0, at X3LYP/cc-pvtz(-f) level.

	ΔG_f^0 (*QM*) (kcal/mol)	ΔG_s^0 (*QM*) (kcal/mol)	ΔG_s^0 (*exp*)[a] (kcal/mol)
Parent compounds			
Water	-53.92	-7.47	-10.5
Formaldehyde	-24.96	-2.89	--
Acetaldehyde	-33.68	-4.17	-3.50
Glyoxal	-45.23	-4.02	--
Acetone	-39.29	-4.97	-3.80
Butanal	-29.06	-3.52	-3.18
Hexanal	-23.72	-3.17	-2.81
Hydrates of			
Formaldehyde	-78.90	-8.94	
Acetaldehyde	-82.19	-12.06	
Acetone	-77.48	-10.90	
Butanal	-77.13	-7.34	
Hexanal	-71.54	-6.23	
β-hydroxycarbonyls of			
Acetaldehyde	-58.17	-10.64	
Acetone	-66.69	-7.78	
Butanal	-45.54	-9.03	
Hexanal	-30.61	-7.78	
α,β-unsaturated carbonyls of			
Acetaldehyde	-12.90	-5.42	
Acetone	-14.89	-4.63	
Butanal	-4.19	-3.88	
Hexanal	9.18	-3.06	

a. Experimental solvation energies are obtained from Wang et al. [34], except for water [21]

Gibbs free energies of reaction for hydration reaction and aldol condensation are calculated (Table 3.3) for both gas, and aqueous phase. Enthalpies of reaction, ΔH_r (gas), are included for reference.

Table 3.3: Quantum calculated enthalpies and Gibbs free energies of reactions for hydration and aldol condensation at T = 298K. All energies are in kcal/mol

	ΔH_r(gas)	ΔG_r(gas)	ΔG_r(aq)
Hydration: Aldehyde + H_2O = Hydrate			
Formaldehyde	-10.81	-0.03	-0.50
Acetaldehyde	-6.31	5.41	3.11
Acetone	4.00	15.73	15.37
Butanal	-5.55	5.85	7.61
Hexanal	-5.73	6.09	8.61
Aldol Condensation: 2 carbonyls = α,β-unsaturated carbonyls + water			
Acetaldehyde	-1.09	0.54	-4.00
Acetone	8.24	9.78	7.61
Butanal	-3.22	0.01	-4.30
Hexanal	0.86	2.70	-1.50

Hydration and aldol condensation are more favorable for aldehydes (formaldehyde, acetaldehyde, butanal, and hexanal) than for acetone, shown by the calculated ΔH_r and ΔG_r. Equilibrium constants (reported as log K) are calculated and shown in Table 3.4. Estimated log K values in liquid solution, log K (liq), where it is assumed that the solution are mostly organic, from Barsanti and Pankow [11, 35] were also in included for reference. The quantum calculated log K values in aqueous solution, log K (aq), follow the same trend as the estimated log K (liq) for both hydration reaction and aldol condensation.

Table 3.4: Quantum calculated log *K* in the gas phase and solution, estimated log K in liquid solution, and experimental log *K* for hydration reaction and aldol condensation at P = 1 atm and T = 298K

	QM log *K* (gas)	QM log *K* (aq)	Barsanti and Pankow [11] log *K* (liq)	Experimental log *K* (aq)
Hydration: Aldehyde + H_2O = Hydrate				
Formaldehyde	0.02	0.36	0.62	
Acetaldehyde	-3.96	-2.28	-6.46	-1.67[a]
Acetone	-11.53	-11.26	-13.72	
Butanal	-4.29	-5.58	-6.55	
Hexanal	-4.47	-6.31	-7.07	
Aldol Condensation: 2 carbonyls = α,β-unsaturated carbonyls + water				
Acetaldehyde	-0.40	2.93	2.22	
Acetone	-7.17	-5.58	-1.79	
Butanal	-0.01	3.15	4.14	
Hexanal	-1.98	1.10	3.34	

a. Calculated from the value of Tur'yan, [36], divided by 55.6 M

Results show that the hydration reactions for most simple aldehydes and ketones (acetone) are unfavorable (Table 3.3). The -0.50 kcal/mol of free energy of hydration for formaldehyde are too small to be considered significant. Kroll et al. [13] has shown that most simple carbonyls (such as formaldehyde and octanal) do not contribute additional OPM via heterogeneous reactions, except glyoxal. Our results seem to support their findings even though the two sets of compounds are mostly different. Experimental thermodynamic data for hydration and aldol condensation of aldehydes and ketones are rare. A study by Tur'yan [36] concluded that the average hydration constant, K_h, for acetaldehyde in bulk solution is 1.19 ± 0.05 (log K_h (aq) = -1.67). Our QM log K_h (aq) = -2.28, showing that the QM result significantly underestimates the extent of hydration for acetaldehyde.

3.5 Uncertainties

QM predicted free energies of reaction, ΔG_r^0(aq), and equilibrium constants (log *K*) remain questionable because of the QM calculated entropies. For "flexible" molecules with low frequency vibrations (such as hexanal), the QM harmonic oscillator approximation is inadequate, and leads to large errors in gas-phase entropies. Additional errors can be caused by neglecting the intermolecular contributions that may be present in the condensed phase. Other issues can arise from multiple conformations of the reactants/products. While a full conformational search is computationally expensive, we have taken a considerable effort in locating the minimum energy conformation. Yet, it is still possible that we have not located the minimum.

An estimation of the uncertainty for the QM prediced ΔG_r^0(aq) is provided instead of error approximation for individual reaction because of the lack of experimental data. The RMS error in heats of formation using the CBHLC method is found to be 2.11 kcal/mol for a set of 50 organic compounds. The RMS error in entropies is estimated to be 1.39 kcal/mol for the 12 compounds in this study, and the RMS error of the solvation energies is found to be 0.9 kcal/mol from the original reference of the implicit continuum solvent model [28]. With these numbers, the uncertainty in ΔG_r^0(aq) for a reaction such as aldol condensation is estimated to be as large as 5.4 kcal/mol.

3.5.1 Glyoxal Reactions

The reaction mechanism for glyoxal heterogeneous reactions in particular matter suggested by Liggio et al. [14] is based on generic hydration and acetal formation. A summary of the reaction pathway is given in Figure 3.2; the whole process was written acid-catalyzed and were supported by the particle mass spectra in their study. They also

suggested that mechanism C to E in Figure 3.2 is more favorable than C to G, agreeing with earlier studies [37-39].

Later studies [13, 16] also observed significant aerosol growth with glyoxal and supported the findings by Liggio et al. [14, 15]. Kroll et al. [13] supported the mass spectra data by Liggio et al. [14, 15] in both masses and intensities, and they both have and suggested that additional pathways are necessary to account for the large glyxoal uptake in the particle phase [13, 15]. Hastings et al. [16] found the threshold humidity and particle growth rate are consistent with Liggio et al. [14] at a glyoxal concentration 4 orders of magnitude difference. The consistency suggests that the gem-diol compound B is highly favored and the surface water on the particle becomes saturated; glyoxal polymerization may therefore proceed at the highest rates. The unique ability of glyxoal to partition into surface water at high concentration may explaine observations by Kroll et al. [13] where additional aerosol growth was only observed for glyoxal.

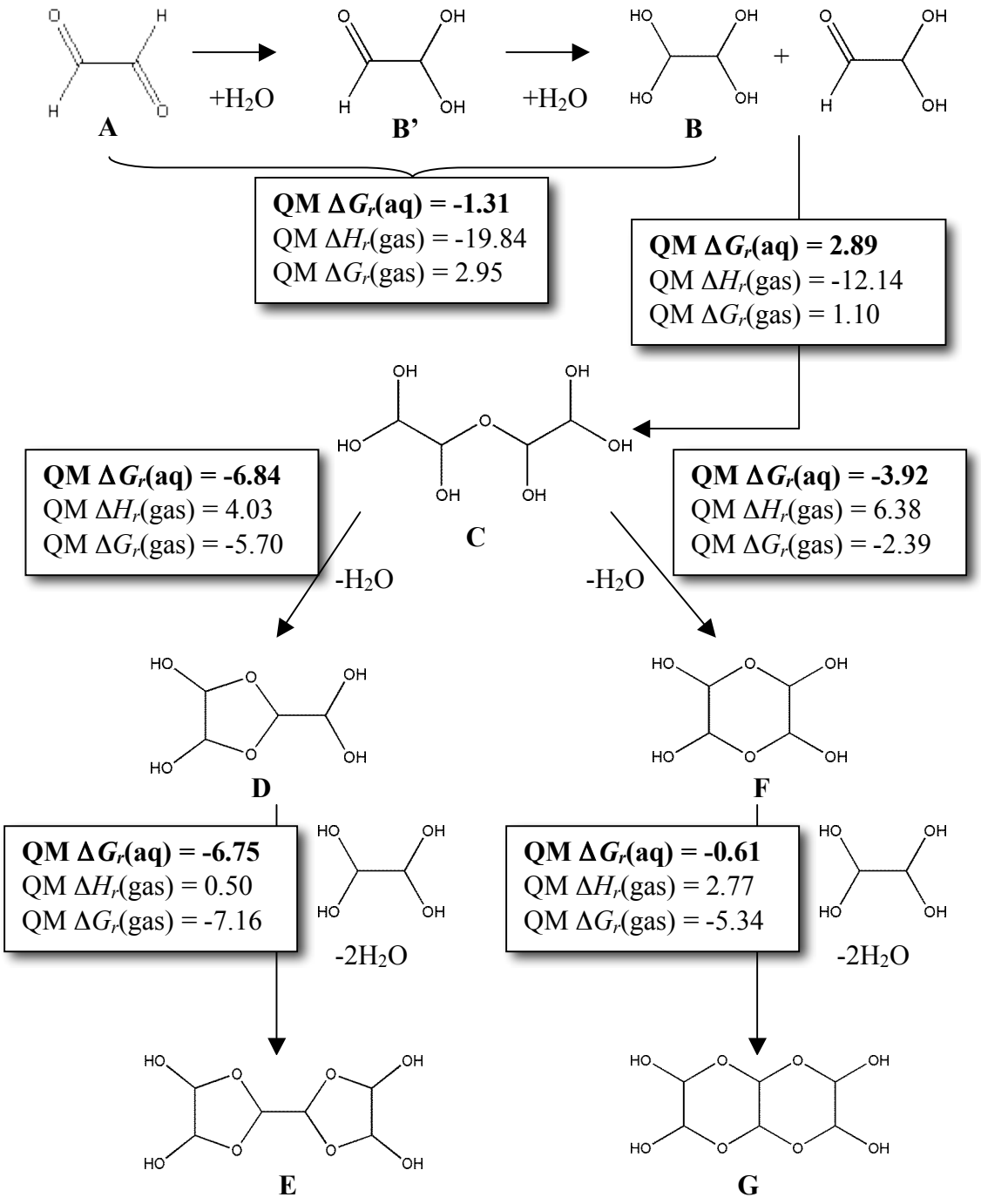

Figure 3.2: A summary of the suggested reaction pathway for glyoxal in particular matter by Liggio et al. [14]. Quantum calculations were done for the proposed structures in the scheme. QM calculated enthalpies and free energies of reactions were shown. All values are in kcal/mol.

Gibbs free energies of reaction, ΔG_r, for the glyoxal reactions in both gas and aqueous phase could be obtained using the computational methods described, ethalphies of reactions are included for reference (Table 3.5).

Table 3.5: Quantum calculated enthalpies (ΔH_f^0) and free energies (ΔG_f^0) of formation, and solvation energies (ΔG_s^0). The structures for compound labeled A – G are shown in Figure 3.2.

Compound	$\Delta H_f^0(QM)$ (kcal/mol)	$\Delta G_f^0(QM)$ (kcal/mol)	$\Delta G_s^0(QM)$ (kcal/mol)
A	-50.65	-45.23	-4.14
B’	-117.63	-98.36	-10.56
B	-184.66	-150.12	-15.34
C	-314.42	-247.39	-21.92
D	-253.31	-199.17	-18.63
E	-323.30	-248.61	-27.26
F	-250.96	-195.86	-18.26
G	-318.68	-243.48	-22.08

As illustrated in Figure 3.2, the free energies of reaction in solution, ΔG_r(aq) have indicated that hydration is favorable. The results are qualitatively consistency with experimental observations, but the number is small and is within the uncertainty estimated (~ 5 kcal/mol). We expect the effect of not including solute-solvent interactions in the condensed phase would be the greatest contributor, as compound B contains 4 hydroxyl groups that may interact with water. The formation of intermediate C is slightly positive, but the subsequent steps in the cyclic acetal formation are favorable enough to compensate. Acetal formation is overall favorable and consistent with experiments. Our results suggest that cyclic acetal formation may proceed with an intermediate other than C. Again, the positive ΔG_r(aq) for B to C are within the uncertainty, so the positive ΔG_r(aq) can be just an artifact caused by the limitations of our QM methods. Our ΔG_r(aq) results, however, have clearly shown that mechanism C to E is preferred over mechanism

C to G, if C can be a valid intermediate compound. To conclude, our quantum calculated results are in qualitative agreement with experimental observations for glyoxal reactions.

All in all, estimation of free energies using quantum methods remains a difficult problem, and the results are quantitatively unreliable. Nevertheless, in the evaluation of thermodynamic tendency of various reactions, where the emphasis is not on the absolute but relative changes in free energies, quantum methods can still serve as useful tools for first approximation, especially for species with no available data. Despite the limitations of the quantum calculations, we have shown that QM results are consistent with experimental observations.

3.6 Acknowledgment

We thank Kelley C. Barsanti at the Department of Environmental and Biomolecular Systems, Oregon Health and Science University for valuable discussions. This work was supported in part by the Electric Power Research Institute.

3.7 Supporting Information

3.7.1 Enthalpies of formation

The ground state energy (E_{elec}), the zero point vibrational energy (E_{zpe}), the thermal vibrational, rotational, and translational enthalpy from 0 K to 298 K ($\Delta H_{(0\text{-}298K)}$) for the selected 12 compounds are summarized in Table 3.6. Molecular structures for these organic compounds are shown in Figure 3.3. QM heats of formation can be calculated using equation 3.3 – 3.5 with the information in Table 3.6. The values are shown in Table 3.8.

Table 3.6: Quantum calculated ground state electronic energies (E_{elec}), zero point energies (E_{zpe}), and thermal enthalpy from 0 - 298K ($\Delta H_{(0\text{-}298K)}$)

	E_{elec} (Hartrees)	E_{zpe} (kcal/mol)	$\Delta H_{(0\text{-}298K)}$(kcal/mol)
Water	-76.44	12.48	2.37
Formaldehyde	-114.50	16.35	2.39
Acetaldahyde	-153.82	33.46	2.95
Acetone	-193.14	50.45	4.02
Butanal	-232.43	68.14	4.59
Hexanal	-311.04	102.27	5.97
Glyoxal	-227.82	22.95	3.23
Ethylene glycol	-230.25	51.80	4.02
Hydroxyacetone	-268.36	54.10	4.55
2,4-pentanedione	-345.77	73.81	5.93
Glutaraldehyde	-345.75	74.21	5.75
Cyclopropane carboxylic acid	-306.46	59.06	4.25

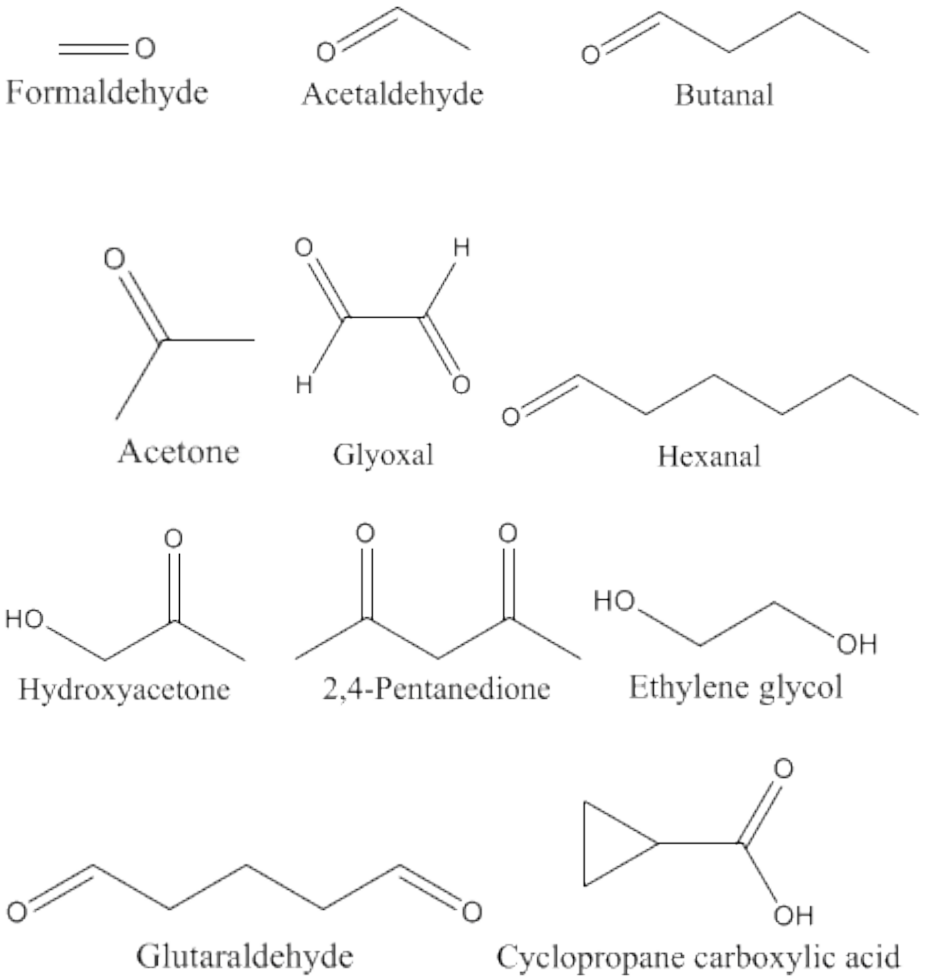

Figure 3.3: Molecular structures of the organic species (formaldehyde, acetaldehyde, acetone, butanal, hexanal, glyoxal, hydroxyacetone, 2,4-pentanedione, ethylene glycol, glutaraldehyde, cyclopropane carboxylic acid) used in the study

3.7.2 CHBLC corrections

However, a direct comparison of QM heats of formation, from Equation 3.3 – 3.5, with the experimental values often shows large errors (see Table 3.8). These errors appear to be highly correlated with the number of carbon or the number of hydrogen atoms in the molecule. Thus, in principle one could attribute the errors in the standard heats of formation to errors in the quantum mechanical ground state electronic energies for the elements. Equation 3.4 is then changed to:

$$\Delta H^{*}_{298K} = \sum_{i=1}^{n} n_i [h_i^0 - (h_i^{QM} - \delta h_i^{elec})] \qquad (3.7)$$

where δh_i^{elec} is the enthalpy correction for the i-th element, 0.61, 0.90, and 0.39 kcal/mol for H, C, and O respectively, somewhat higher, 2.84 and 4.80 kcal/mol, for S and N, see Table 3.7. Substituting these values in equation (3.7) lead to a root mean square deviation of ~ 1.7 kcal/mol for the standard heats of formation of 34 hydrocarbons, nitrogen and sulfur containing organic compounds in the work of Blanco and Goddard [23].

Table 3.7: Experimental (h_i^0) and calculated (h_i^{QM}) atomic heats of formation, and the quantum corrections to heats of formation (δh_i^{elec})

Atom	h_i^0 (kcal/mol)[a]	h_i^{QM} (Hartrees)[b]	δh_i^{elec} (kcal/mol)[c]
H (^{2}S)	52.07	-0.501	-0.61
C (^{3}P)	171.18	-37.841	-0.90
N (^{4}S)	112.90	-54.588	-4.80
O (^{3}P)	59.51	-75.067	-0.39
S (^{3}P)	66.20	-398.086	2.84

a. The experimental heats of formation, h_i^0, and the experimental atomic entropy are taken from NIST database [21].
b. Theoretical atomic heats of formation are calculated at X3LYP/aug-ccpvtz(-f) level
c. Corrections to atomic enthalpies are developed according to Blanco and Goddard [23]

Further corrections can be electron correlated, particularly for valence electrons. A simple classification of valence bond (VB) electron pairs into σ and π electron pairs provides an effective systematic correction, similar to the J2 model [22]. Equation 3.7 is then changed to:

$$\Delta H^{*}_{298K} = \sum_{i=1}^{n} n_i [h_i^0 - (h_i^{QM} - \delta h_i^{elec})] + \sigma N_\sigma + \pi N_\pi \qquad (3.8)$$

where N_σ and N_π are the number of σ and π electron pairs in each compound respectively. For a set of 50 compounds of hydrocarbons, S, N and O containing

compounds, we found σ = -2.36 and π = -0.022 kcal/mol. (For J2P3 method, σ = -1.2 and π = -4.8 kcal/mol) Corrected predictions versus experimental standard heats of formation (298.15 K, 1 atm) are shown to have a RMS deviation for standard heats of formation of 2.11 kcal/mol for a total 50 organic compounds. The original CBHLC corrections are developed targeting oil migration distance indicators such as dibenzothiophenes and methylcarbazoles (only C, H, S and N containing compounds). For this study, the CBHLC method is extended to oxygenates using 14 oxygen-containing compounds (water, 1,4-cyclohexanedione, benzaldehyde, acetone, butanol, 1,2-dihydroxynaphthalene, ethyl decanoate, hexanoic acid, glyoxal, acetaldehyde, butanal, 2,4-pentanedione, hexanal, and decanol)

Table 3.8: Quantum calculated heats of formation with and without CBHLC. The experimental heats of formation are included for comparison, and the absolute errors (δH) are also shown. All values are in kcal/mol

	ΔH_f^0 (*exp*)[a]	ΔH_f^0 (*QM*) using eq. 3 - 5	δH[e]	CBHLC corrected ΔH_f^0 (*QM*)	δH[e]
Water	-57.80 ± 0.0096	-53.96	3.83	-57.08	0.71
Formaldehyde	-25.96 ± 0.5	-21.82	4.14	-26.42	-0.46
Acetaldehyde	-40.77 ± 1.50	-32.40	8.38	-41.96	-1.19
Acetone	-52.23 ± 0.14	-39.81	12.42	-54.34	-2.11
Butanal	-50.61 ± 0.22	-32.45	18.16	-51.95	-1.34
Hexanal	-59.38 ± 1.78[b]	-33.13	26.25	-62.56	-3.19
Glyoxal	-50.64 ± 0.79[c]	-42.60	8.04	-50.65	-0.01
Ethylene glycol	-94.20 ± 0.67	-76.74	17.46	-91.77	2.43
Hydroxyacetone	-87.42 ± 8.74[b]	-73.89	13.52	-90.40	-2.98
2,4-Pentanedione	-91.87 ± 0.31	-65.46	26.41	-88.41	3.46
Glutaraldehyde	-73.49 ± 3.67[b]	-51.05	22.44	-74.00	-0.51
Cyclopropane carboxylic acid	-80.30 ± 4.01[b]	-57.85	22.45	-78.17	2.13

a. Experimental values and uncertainties of heats of formation, ΔH_f^0 (*exp*) are obtained from NIST webbook [21]. Original references for water [40], formaldehyde [41], acetaldehyde, acetone, and butanal [42], ethylene glycol [43] and 2,4-pentanedione [44]
b. Experimental values heats of formation, ΔH_f^0 (*exp*) are obtained from DIPPR database [32] for hexanal, hydroxyacetone, glutaraldehyde and cyclopropane carboxylic acid.
c. Glyoxal data are obtained from Dorofeeva et al. [45]
d. $\delta H = \Delta H_f^0$ (*QM*) - ΔH_f^0 (*exp*)

3.7.3 Standard Entropies

Standard entropies of the molecules from quantum mechanics were used to calculate free energies of formation (ΔG^0_f) and reaction (ΔG^0_{rxn}). Quantum reported gas-phase entropies and experimental entropies [21, 32, 45] are shown in Table 3.9.

Table 3.9: Reported entropies from quantum mechanics, $S^0_{298K}(QM)$, experimental entropies, S^0. Absolute errors (δS) are shown, and all values are in cal/mol K

	S^0 (exp)[a]	$S^0_{298K}(QM)$	δS[d]
Water	45.13 ± 0.0024	45.085	-0.05
Formaldehyde	52.25	52.148	-0.10
Acetaldehyde	63.04	61.813	-1.23
Acetone	70.57	71.663	1.09
Butanal	82.11 ± 2.46	77.901	-4.20
Hexanal	100.83 ± 3.02[b]	89.494	-11.33
Glyoxal	65.09 ± 0.72[c]	64.714	-0.37
Ethylene glycol	74.48	70.291	-4.19
Hydroxyacetone	81.92 ± 8.19[b]	78.355	-3.57
2,4-pentanedione	86.58 ± 0.87[b]	91.188	4.61
Glutaraldehyde	97.04 ± 4.85[b]	88.646	-8.40
Cyclopropane carboxylic acid	74.95 ± 2.25[b]	76.282	1.33

a. Experimental values and uncertainties of entropies, S^0(exp) are obtained from NIST webbook [21]. Original references for water [40], formaldehyde [41], acetaldehyde, and acetone [42], butanal [46], ethylene glycol [47].
b. For hexanal, hydroxyacetone, 2,4-pentanedione, glutaraldehyde, and cyclopropane carboxylic acid, S_f^0(exp) and the uncertainties are taken from DIPPR database [32].
c. Glyoxal data are obtained from Dorofeev et al. [45].
d. $\delta S = S^0$ (QM) - S^0 (exp)

3.7.4 Standard states conversion

In order to convert from gas-phase standard condition to solution-phase condition, we can employ the basic equation:

$$\Delta G^{0'} = \Delta G^0 + RT \ln\left(\frac{Q^{0'}}{Q^0}\right) \qquad (3.9)$$

where Q is the reaction quotient, the ratio of concentrations that appear in the equilibrium constant. For a reaction such as hydration (carbonyl + water = hydrate), the reaction quotient, Q, can be written as [hydrate]/[carbonyl][water]. To convert the gas-phase standard state (1 atm) concentration to solution phase standard concentration (1 M), we will define the $Q^{0\prime}$and $\Delta G^{0\prime}$ as values evaluated with all species at 1 atm, while Q^0 and

ΔG^0 are evaluated in the gas phase with all species at 1M. Assuming the species are ideal gases, their concentrations may be obtained from the ideal gas law as 1/24.5 M [17]. For a reaction such as hydration,

$$\Delta G^0(\text{gas, 1M}) = \Delta G^{0'}(\text{gas, 1atm}) - RT\ln(24.5) \qquad (3.10)$$

3.7.5 Solvation energy

Solvation energy refers to the change in free energy for a molecular A leaving the gas phase and entering the condensed phase. This free energy can be determined using

$$\Delta G_S^0(A) = \lim_{[A]_{sol}\to 0}\left\{-RT\ln\frac{[A]_{sol}}{[A]_{gas}}\bigg|_{eq}\right\} \qquad (3.11)$$

When a solute is immersed in a solvent, its charge distribution interacts with that of the solvent [17], and how to treat the solvation effect efficiently and accurately is a long-term challenge in computational chemistry. The solvation model employed in this study is based on the Poisson-Boltzmann (PB) equation.

$$\nabla\varepsilon(\mathbf{r})\cdot\nabla\phi(\mathbf{r}) - \varepsilon(\mathbf{r})\lambda(\mathbf{r})\kappa^2\frac{k_BT}{q}\sinh\left[\frac{q\phi(\mathbf{r})}{k_BT}\right] = -4\pi\rho(\mathbf{r}) \qquad (3.12)$$

The charge density ρ of the solute may be expressed as some continuous function of $\mathbf{r}$. ε is the dielectric constant of the medium, ϕ is the electrostatic potential, λ is the simple switching function with is zero in regions inaccessible to electrolyte and one otherwise. q is the charge of the electrolyte ions, and κ^2 is the Debye-Hückel parameter given by

$$\kappa^2 = \frac{8\pi q^2 I}{\varepsilon k_B T} \qquad (3.13)$$

where I is the ionic strength. Solving the PB equation can be quite complicated and usually involves additional assumptions. At low ionic strength it is given as a linearized PB equation using a truncated power expansion for the hyperbolic sine,

$$\nabla\varepsilon(\mathbf{r})\cdot\nabla\phi(\mathbf{r}) - \varepsilon(\mathbf{r})\lambda(\mathbf{r})\kappa^2\phi(\mathbf{r}) = -4\pi\rho(\mathbf{r}) \qquad (3.14)$$

The solvation model in this study is limited by zero ionic strength, the PB equation can be reduced to Poisson equation and can be solved relatively easier. Details of the computational procedure of the solvation model in this study can be found in the original reference Tannor et al. [28].

3.8 References

1. Seinfeld, J. H.; Pankow, J. F., Organic aerosol particular metter. *Ann. Rev. Phys. Chem.* **2003,** *54*, 121.140.

2. Pankow, J. F.; Seinfeld, J. H.; Asher, W. E.; Erdakos, G. B., Modeling the formation of secondary organic aerosol. 1. Application of theoretical principles to measurements obtained in the α-pinene, β-pinene, sabinene, Δ^3-carene, and cyclohexene-ozone systems. *Environmental Science and Technology* **2001,** *35*, (6), 1164-1172.

3. Seinfeld, J. H.; Erdakos, G. B.; Asher, W. E.; Pankow, J. F., Modeling the formation of secondary organic aerosol (SOA). 2. The predicted effects of relative humidity on aerosol formation in the α-pinene, β-pinene, sabinene, Δ^3-carene, and cyclohexene-ozone systems. *Environmental Science and Technology* **2001,** *35*, (9), 1806-1817.

4. Pankow, J. F., An absorption model of the gas/particle partitioning involved in the formation of secondary organic aerosol. *Atmospheric Environment* **1994,** *28*, 189-193.

5. Pankow, J. F., An absorption model of gas/particle partitioning of organic compounds in the atmosphere. *Atmospheric Environment* **1994,** *28*, 185-188.

6. Gao, S.; Ng, N. L.; Keywood, M.; Varutbangkul, V.; Bahreini, R.; Nenes, A.; He, J.; Yoo, K. Y.; Beauchamp, J. L.; Hodyss, R. P.; Flagan, R. C.; Seinfeld, J. H., Particle phase acidity and oligomer formation in secondary organic aerosol. *Environmental Science and Technology* **2004,** *38*, (24), 6582-6589.

7. Koehler, C. A.; Fillo, J. D.; Ries, K. A.; Sanchez, J. T.; De Haan, D. O., Formation of secondary organic aerosol by reactive condensation of furandiones,

aldehydes, and water vapor onto inorganic aerosol seed particles. *Environmental Science and Technology* **2004,** *38*, (19), 5064-5072.

8. Jang, M.; Czoschke, N. M.; Lee, S.; Kamens, R. M., Heterogeneous atmospheric organic aerosol production by acid-catalyzed particle-phase reaction. *Science* **2002,** *298*, 814-817.

9. Jang, M.; Kamens, R. M., Atmospheric secondary aerosol formation by heterogeneous reactions of aldehydes in the presence of a sulfuric acid aerosol catalyst. *Environmental Science and Technology* **2001,** *35*, 4758-4766.

10. Jang, M. S.; Kamens, R. M., Characterization of secondary aerosol from the photo-oxidation of toluene in the presence of NOx and 1-propene. *Environmental Science and Technology* **2001,** *35*, (18), 3626-3639.

11. Barsanti, K. C.; Pankow, J. F., Thermodynamics of the formation of atmospheric organic particulate matter by accretion reactions - Part 1: aldehydes and ketones. *Atmospheric Environment* **2004,** *38*, (26), 4371-4382.

12. Barsanti, K. C.; Pankow, J. F., Thermodynamics of the formation of atmospheric organic particulate matter by accretion reactions - 2. Dialdehydes, methylglyoxal, and diketones. *Atmospheric Environment* **2005,** *39*, 6597-6607.

13. Kroll, J. H.; Ng, N. L.; Murphy, S. M.; Varutbangkul, V.; Flagan, R. C.; Seinfeld, J. H., Chamber studies of secondary organic aerosol growth by reactive uptake of simple carbonyl compounds. *Journal of Geophysical Research* **2005,** *110*, D23207.

14. Liggio, J.; Li, S.-M.; McLaren, R., Heterogeneous reactions of glyoxal on particulate matter: Identification of acetals and sulfate esters. *Environmental Science and Technology* **2005,** *39*, 1532-1541.

15. Liggio, J.; Li, S.-M.; McLaren, R., Reactive uptake of glyoxal by particulate matter. *Journal of Geophysical Research* **2005,** *110*, D10304.

16. Hastings, W. P.; Koehler, C. A.; Bailey, E. L.; De Haan, D. O., Secondary organic aerosol formation by glyoxal hydration and oligomer formation: Humidity effects and equilibrium shifts during analysis. *Environmental Science and Technology* **2005,** *39*, 8728-8735.

17. Cramer, C. J., *Essentials of Computational Chemistry: Theories and Models*. 2nd ed.; Wiley: 2004.

18. Kendall, R. A.; Dunning Jr, T. H.; Harrison, R. J., Electron affinities of the first-row atoms revisited. Systematic basis sets and wave functions. *Journal of Chemical Physics* **1992,** *96*, (9), 6796-6806.

19. Hariharan, P. C.; Pople, J. A., Effect of d-functions on molecular orbital energies for hydrocarbons. *Chemical Physics Letters* **1972,** *16*, (2), 217-219.

20. Scott, A. P.; Radom, L., Harmonic vibrational frequencies: An evaluation of Hartree-Fock, Moller-Plesset, Quadratic configuration interaction, Density functional theory, and Semiempirical scale factors. *Journal of Physical Chemistry* **1996,** *100*, 16502-16513.

21. Linstrom, P. J.; Mallard, W. G., *NIST Chemistry WebBook, NIST Standard Reference Database Number 69*. National Institute of Standards and Technology (http://webbook.nist.gov): Gaithersburg MD, 2003.

22. Dunietz, B. D.; Murphy, R. B.; Friesner, R. A., Calculation of atomization energies by multiconfigurational localized perturbation theory - Application for closed shell cases. *Journal of Chemical Physics* **1999,** *110*, (4), 1921-1930.

23. Blanco, M.; Goddard III, W. A., Thermal concentration drifts in molecular indicators of secondary oil migration from accurate quantum mechanics. *Journal of Physical Chemistry A* **2005,** *(Submitted)*.

24. *Jaguar 6.0*, Schrodinger, L L C: Portland, OR, 2005.

25. Xu, X.; Goddard III, W. A., The X3LYP extended density functional for accurate descriptions of nonbond interactions, spin states, and thermochemical properties. *Proceedings of the National Academy of Sciences of the United States of America* **2004,** *101*, (9), 2673-2677.

26. Xu, X.; Goddard III, W. A., Bonding properties of the water dimer: A comparative study of density functional theories *Journal of Physical Chemistry A* **2004,** *108*, (12), 2305-2313.

27. Su, J. T.; Xu, X.; Goddard III, W. A., Accurate energies and structures for large water clusters using the X3LYP hybrid density functional. *Journal of Physical Chemistry A* **2004,** *108*, (47), 10518-10526.

28. Tannor, D. J.; Marten, B.; Murphy, R. B.; Friesner, R. A.; Sitkoff, D.; Nicholls, A.; Ringnalda, M. N.; Goddard III, W. A.; Honig, B., Accurate first principles calculation of molecular charge-distributions and solvation energies from ab initio quantum mechanics and continuum dielectric theory. *Journal of American Chemical Society* **1994,** *116*, (26), 11875-11882.

29. Honig, B.; Nicholls, A., Classical electrostatics in biology and chemistry. *Science* **1995,** *268*, 1144-1149.

30. Marten, B.; Kim, K.; Cortis, C.; Friesner, R. A.; Murphy, R. B.; Ringnalda, M. N.; Sitkoff, D.; Honig, B., New model for calculation of solvation free energies:

correction of self-consistent reaction field continuum dielectric theory for short-range hydrogen bonding effects. *Journal of Physical Chemistry* **1996,** *100*, (28), 11775-11788.

31. Reid, R. C.; Prausnitz, J. M.; Poling, B. E., *Properties of Gases and Liquids*. 4th ed.; McGraw-Hill: New York, 1987.

32. Daubert, T. E.; Danner, R. P. Data Compilation of Pure Compound Properties, Technical Database Services.

33. Yaws, C. L., *Chemical Properties Handbook*. McGraw-Hill: New York, 1999.

34. Wang, J.; Wang, W.; Huo, S.; Lee, M.; Kollman, P. A., Solvation model based on weighted solvent accessible surface area. *Journal of Physical Chemistry B* **2001,** *105*, 5055-5067.

35. Sum, A. K.; Sandler, S. I.; Bukowski, R.; Szalewicz, K., Prediction of the phase behavior of acetonitrile and methanol with ab initio pair potentials. I. Pure components. *Journal of Chemical Physics* **2002,** *116*, (17), 7627-7636.

36. Tur'yan, Y. I., Studying kinetics of the dehydration reaction of acetaldehyde in aqueous solution using polarographic kinetic currents. *Coratica Chemica Acta* **2000,** *73*, (3), 657-666.

37. Fratzke, A. R.; Reilly, P. J., Kinetic-analysis of the disproportionation of aqueous glyoxal. *International Journal of Chemical Kinetics* **1986** *18*, (7), 757-773.

38. Fratzke, A. R.; Reilly, P. J., Thermodynamic and kinetic-analysis of the dimerization of aqueous glyoxal. *International Journal of Chemical Kinetics* **1986,** *18*, (7), 775-789.

39. Whipple, E. B., Structure of glyoxal in water. *Journal of American Chemical Society* **1970,** *92*, (24), 7183-7186.

40. Cox, J. D.; Wagman, D. D.; Medvedev, V. A., *CODATA Key Values for Thermodynamics* Hemisphere Publishing Corp.: New York, 1984.

41. Gurvich, L. V.; Veyts, I. V.; Alcock, C. B., *Thermodynamic Properties of Individual Substances*. Forth ed.; Hemispheric Publishing Company: New York, 1989.

42. Wiberg, K. B.; Crocker, L. S.; Morgan, K. M., Thermochemical studies of carbonyl compounds. 5. Enthalpies of reduction of carbonyl groups. *Journal of American Chemical Society* **1991,** *113*, 3447-3450.

43. Knauth, P.; Sabbah, R., Energies of intra- and intermolecular bonds in w-alkanediols (II) Thermochemical study of 1,2-ethanediol, 1,3-propanediol, 1,4-butanediol, and 1,5-pentanediol at 298.15K. *Structural Chemistry* **1990,** *1*, 43-46.

44. Hacking, J. M.; Pilcher, G., Enthalpy of combustion of pentane-2,4-dione. *Journal of Chemical Thermodynamics* **1979,** *11*, 1015-1017.

45. Dorofeeva, O.; Novikov, V. P.; Neumann, D. B., NIST-JANAF Thermochemical Tables. I Ten organic molecules related to atmospheric chemistry. *Journal of Physical Chemistry Reference Data* **2001,** *30*, (2), 475-513.

46. Chermin, H. A. G., Thermo Data for petrochemicals. Part 27: Gaseous normal aldehydes. The important thermo properties are presented for all the gaseous normal aldehydes from formaldehyde through decaldehdye *Pet. Refin.* **1961,** *40*, 181-184.

47. Chao, J., Thermodynamic properties of key organic oxygen compounds in the carbon range C1 to C4. Part 2. Ideal gas properties. *Journal of Physical Chemistry Reference Data* **1986,** *15*, 1369-1436.